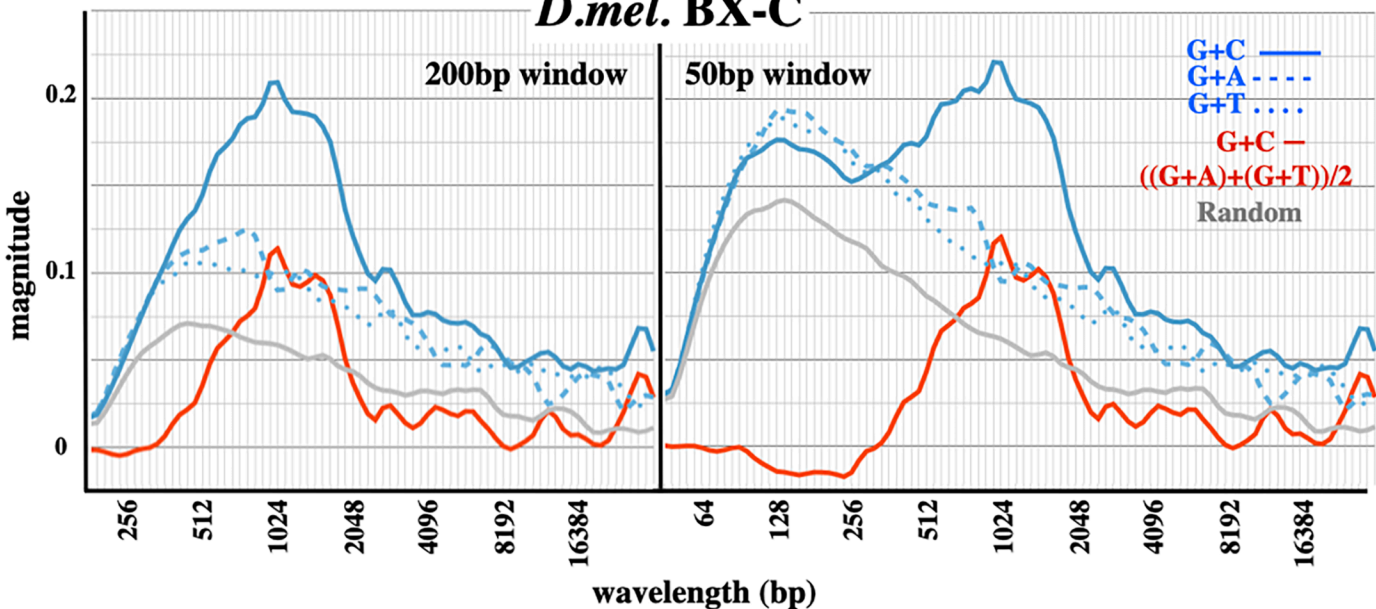
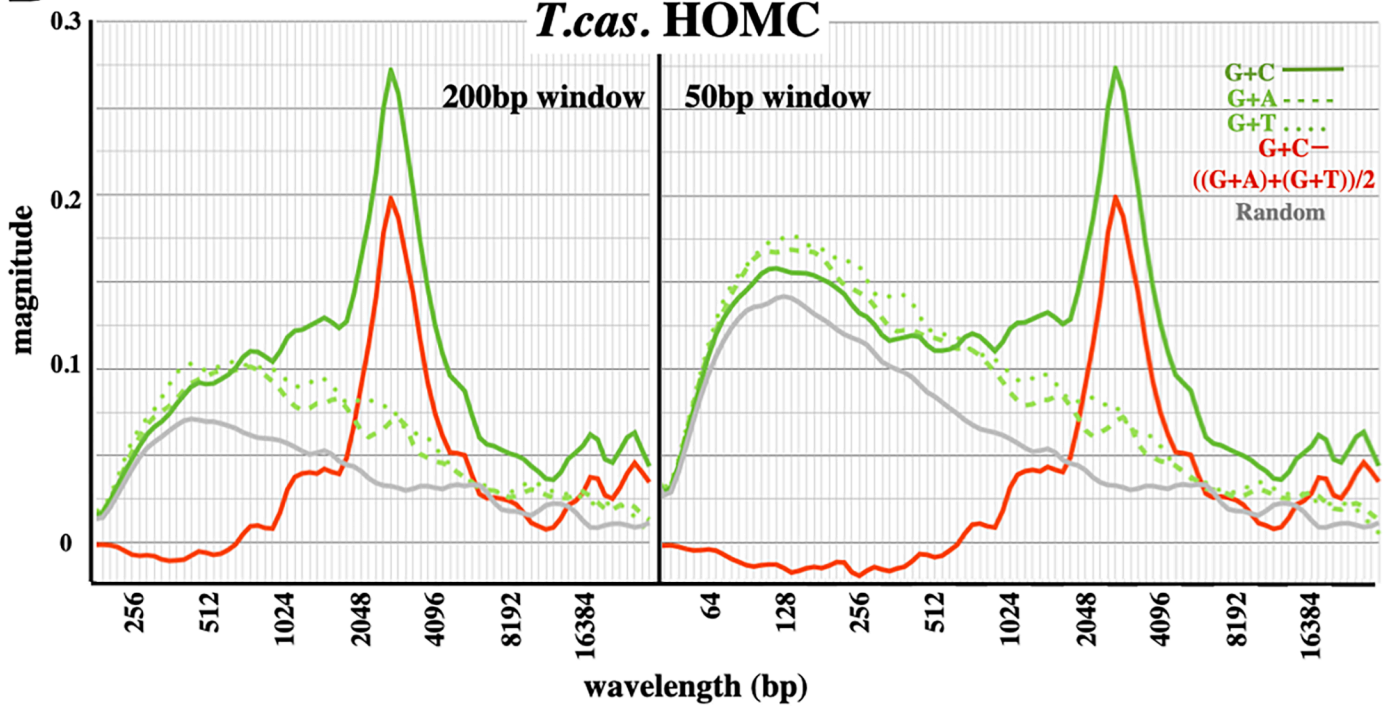
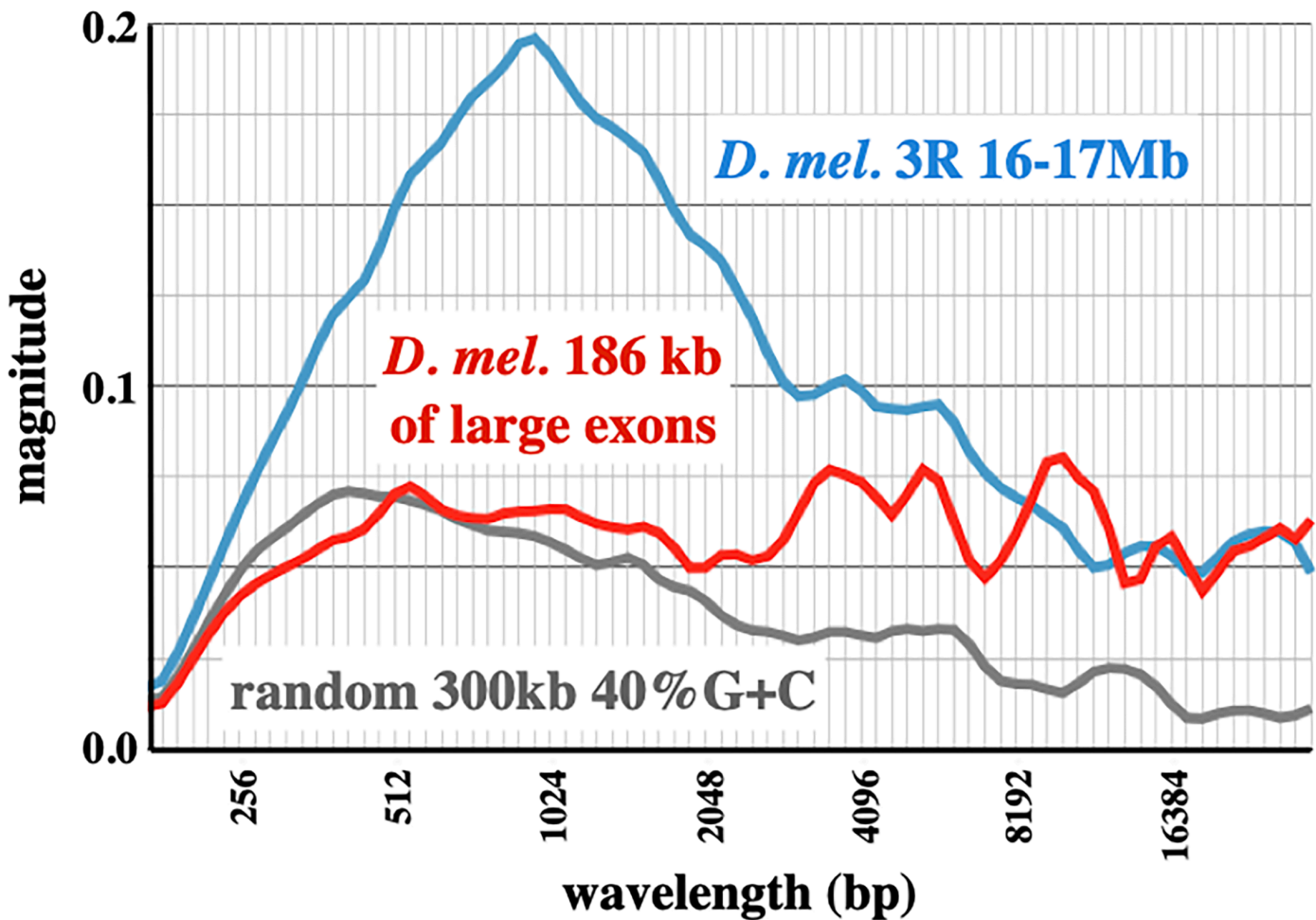


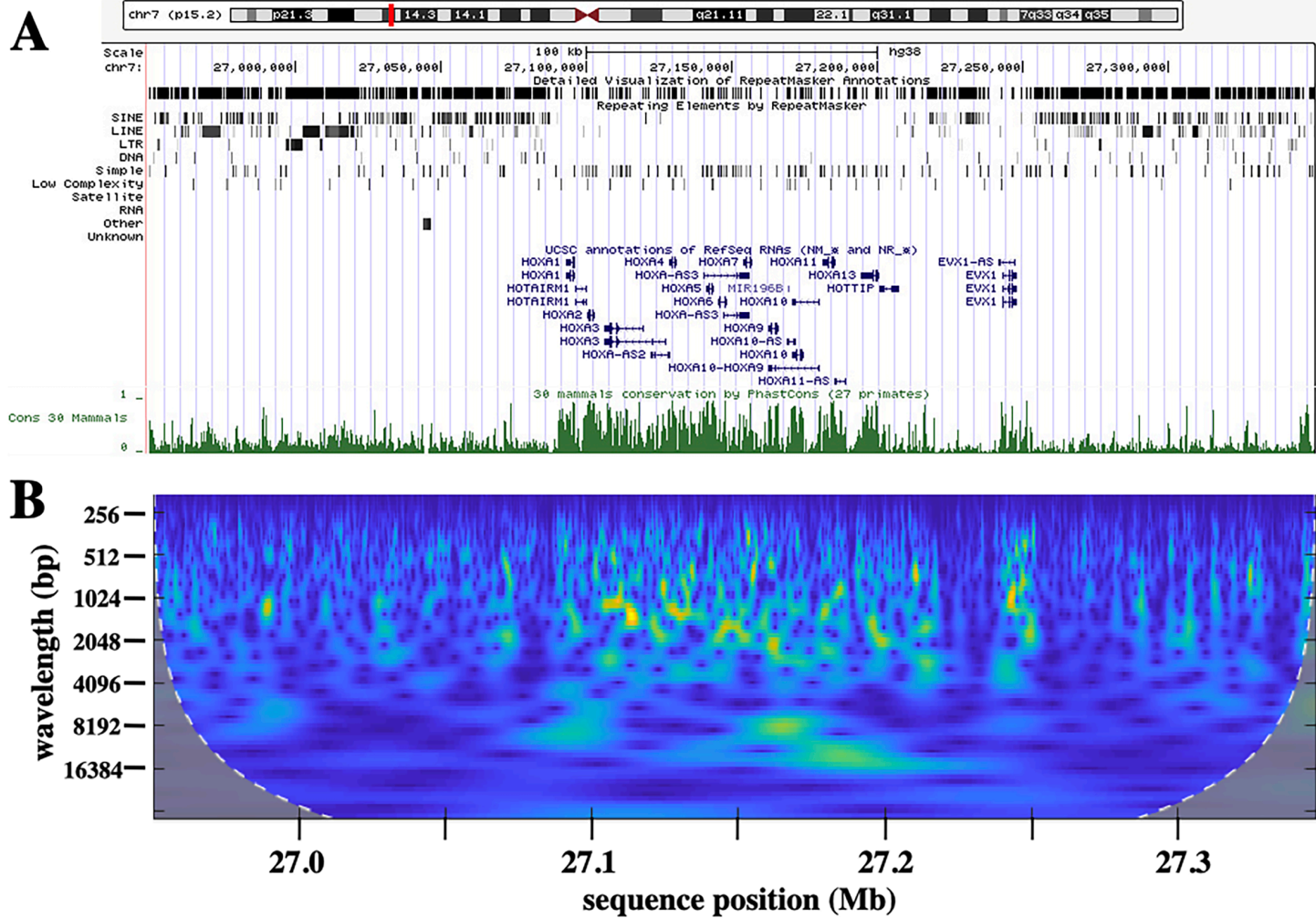
A***D.mel.* BX-C****B*****T.cas.* HOMC****Supplemental Fig. S1**

Magnitude plots for different pairs of bases for the random, fly, and beetle sequences of Figures 2 and 3. Sequences are averaged across 200 bp windows (left) or 50 bp windows (right). The plots for G+A and G+T are similar between species, and are greater in magnitude than those for the randomly shuffled sequence (whose plots are virtually identical for all pairs), but they lack the peaks apparent for G+C. The red lines show the differential oscillation magnitudes for G+C above the averages of G+A and G+T; these show sharper peaks than those of the starting G+C plots.



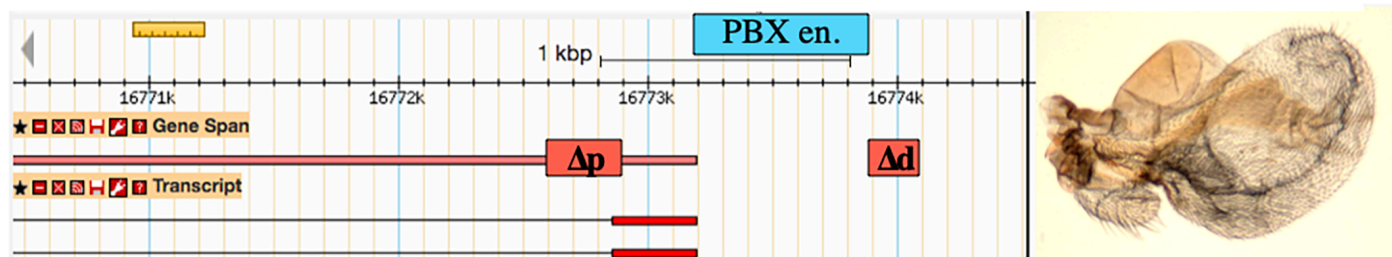
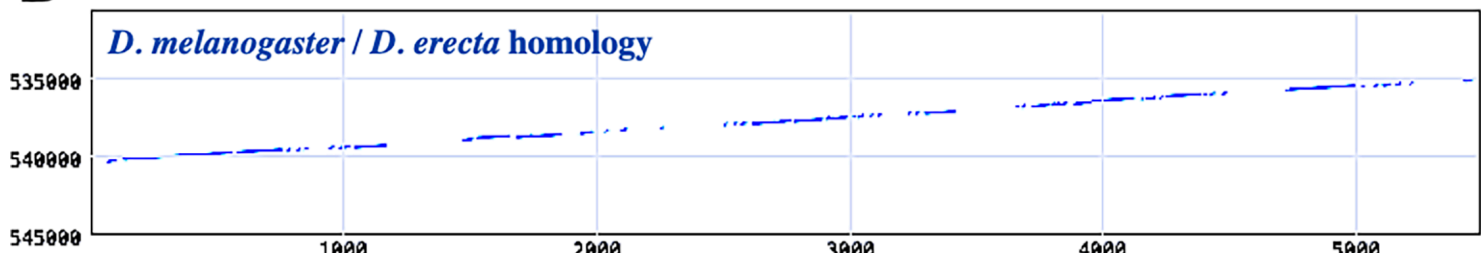
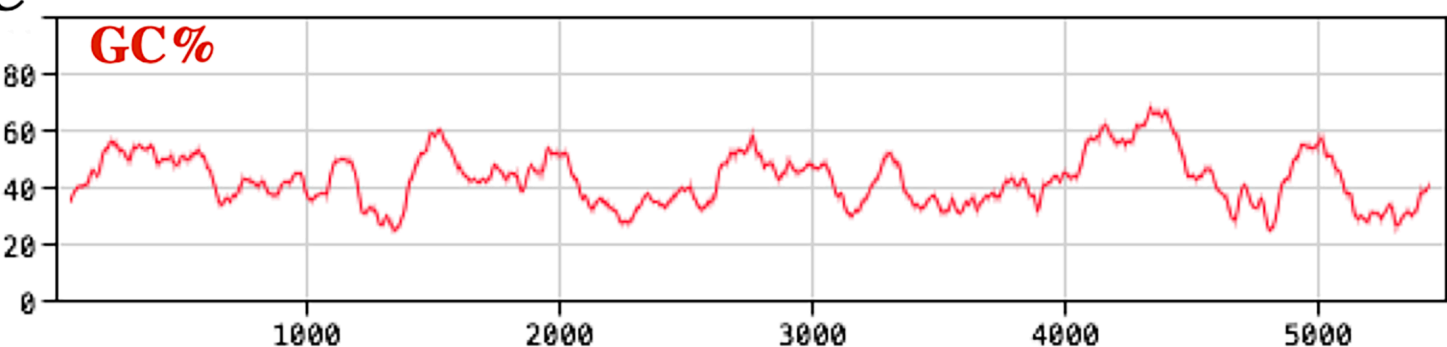
Supplemental Fig. S2

Minimal GC% oscillation in coding sequences. Thirty-three large coding exons from *D. melanogaster* genes, ranging from 3.5 to 12 kb, were aggregated into a 186 kb sequence file, with an overall 51% G+C content. This file was analyzed with the continuous wavelet transform, using a 200 base sliding window. The resulting magnitude graph is compared with that of 1 Mb of genomic DNA, copied from Fig. 4A. The coding sequence approximates our randomly shuffled sequence in the 200-2000bp range; the larger magnitudes at longer wavelengths likely reflect the juxtapositions of unrelated exons.



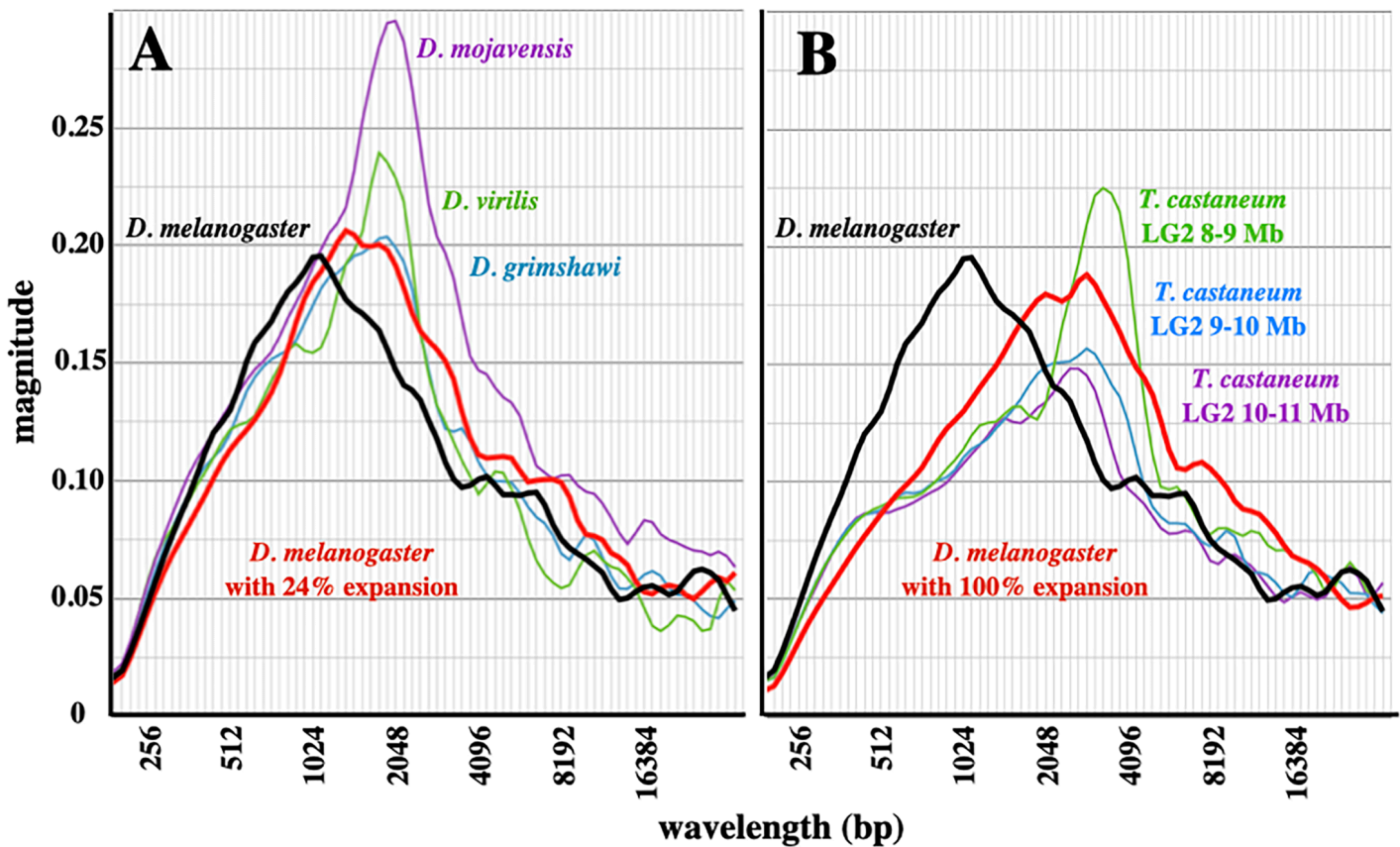
Supplemental Fig. S3

Oscillation in conservation in a human Hox locus. **A.** UCSC Genome Browser screen shot of a 400 kb region of human Chromosome 7 including the HoxA locus. The middle portion, covering the *HoxA1* through *HoxA13* transcription units, is relatively depleted of mobile elements (top) and relatively well conserved in relation to other mammals (green histogram at bottom). **B.** A cwt heatmap of phastCons scores for the same 400 kb region shows higher magnitude (green to yellow coloring), in the 1-2 kb wavelength range, across both the Hox genes and the adjacent EVX1 locus. Removal of the Hox gene exons from the analysis does not significantly alter the heatmap, except that it reduces the signal at wavelengths larger than 8 kb.

A**B****C**

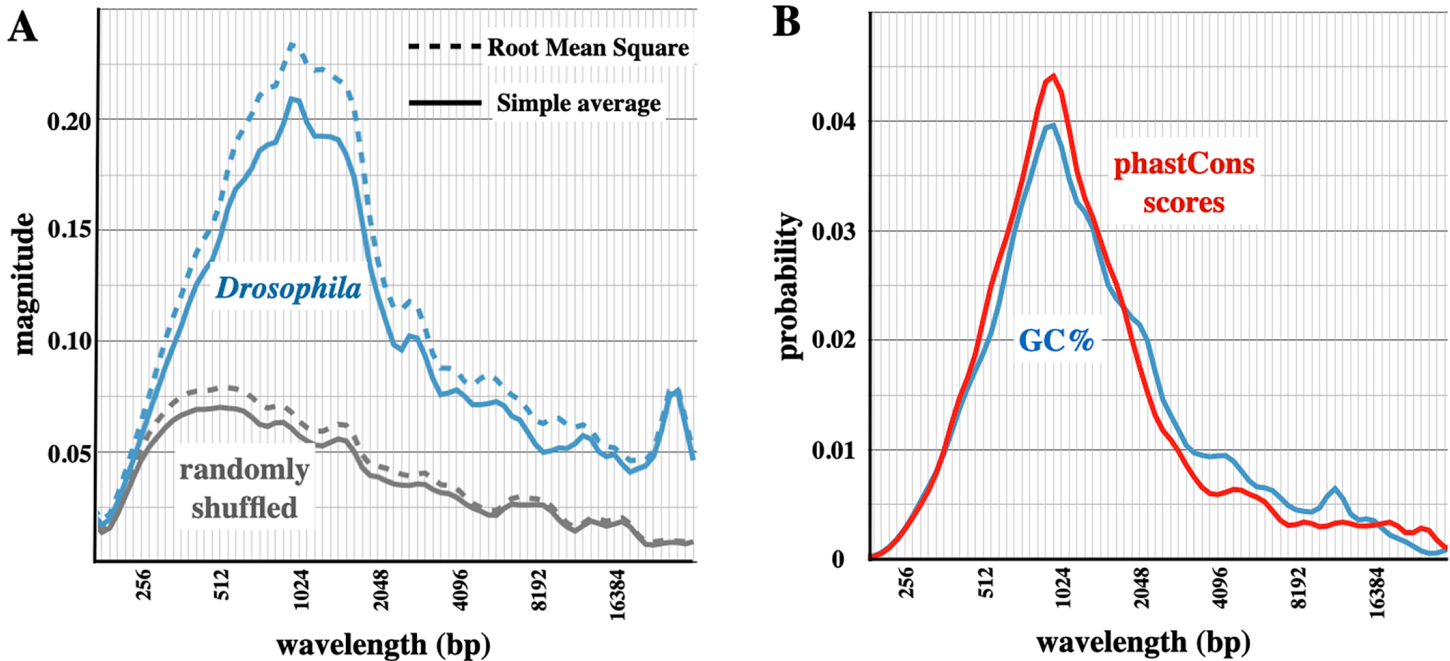
Supplemental Fig. S4

Crowding the Drosophila PBX enhancer. **A.** A map from GBrowse (flybase.org) showing a ~5 kb region of the *D. melanogaster* bithorax complex centered on the PBX enhancer. A non-coding RNA initiates adjacent to the enhancer and extends to the left. The blue box shows a 713 base segment that deletes the core PBX enhancer, which was previously defined by reporter constructs (Pirrotta et al. (1995)). The inset shows a posterior haltere-to-wing transformation of a fly homozygous for this deletion. The red boxes flanking the core enhancer (Δp and Δd) show proximal and distal sequence segments that were separately deleted on an otherwise wild-type chromosome. **B.** The deleted regions correspond to segments of poor conservation (shown in a Pustell dot matrix comparison of *D. melanogaster* and *D. erecta*). **C.** G+C content of the region, here averaged with a 100 bp sliding window. The deleted regions also correlate to segments of low GC%. Flies homozygous for either the Δp or the Δd deletion show no apparent segmental transformations. Flies heterozygous for either Δp or Δd over a large deficiency for the region (*Df(3R)P10*) are indistinguishable from + / *Df P10*.



Supplemental Fig. S5

Random addition model. **A.** Randomized 10-bp blocks with a 30% G+C content were added to a 1 Mb sequence of *D. melanogaster* (chromosome 3R, 16-17 Mb), with insertions restricted to sequence regions with less than 31.2% G+C. Additions were continued until the total sequence measured ~1.24 Mb. The magnitude graph of GC% oscillation in this model sequence (in red) is compared with the spectra of the starting *D. melanogaster* sequence (black) and of partially homologous sequences from *D. virilis*, *D. grimshawi*, and *D. mojavensis*. **B.** The same *D. melanogaster* sequence was similarly expanded to 2 Mb. The resulting magnitude graph is plotted against the starting *D. melanogaster* graph, and with graphs from three adjacent 1 Mb segments of *T. castaneum* LG2.



Supplemental Fig. S6

Alternative plots. **A.** Comparison of magnitude graphs computed as a simple average or root mean square. The sequence from *D. melanogaster* Chr. 3R 16.66-16.96 Mb, as used in Fig. 2 and Fig. 3, is analyzed. Solid lines show simple averaging of cwt magnitudes as a function of wavelength, as was done for Fig. 3 and other magnitude graphs. Dashed lines represent the root mean square of the magnitude scores, i.e. $\sqrt{(\sum_1^n x^2) / n}$. This method is often used in signal processing, but it gives higher values than the average magnitudes. **B.** Recalculation of the data used in Fig. 6B, here using the MATLAB timeSpectrum function normalized with a probability density function. The plots for GC% and phastCons scores are even more coincident, but the probability scores cannot be compared with the magnitudes of Fig. 6B.